Studies of B^0-$\overline{B}^0$ mixing properties with inclusive dilepton events

N. C. Hastings,[21] K. Abe,[8] K. Abe,[42] R. Abe,[28] T. Abe,[43] I. Adachi,[8] H. Aihara,[44] M. Akatsu,[22] Y. Asano,[49] T. Aso,[48] V. Aulchenko,[1] T. Aushev,[12] A. M. Bakich,[39] Y. Ban,[32] E. Banas,[26] A. Bay,[18] I. Bedny,[1] I. Bizjak,[13] A. Bondar,[1] A. Bozek,[26] M. Bračko,[20,13] J. Brodzicka,[26] T. E. Browder,[7] B. C. K. Casey,[7] M.-C. Chang,[25] P. Chang,[25] Y. Chao,[25] K.-F. Chen,[25] B. G. Cheon,[38] R. Chistov,[12] S.-K. Choi,[6] Y. Choi,[38] Y. K. Choi,[38] M. Danilov,[12] L. Y. Dong,[10] A. Drutskoy,[12] S. Eidelman,[1] V. Eiges,[12] Y. Enari,[22] C. W. Everton,[21] F. Fang,[7] C. Fukunaga,[46] N. Gabyshev,[8] A. Garmash,[1,8] T. Gershon,[8] B. Golob,[19,13] J. Haba,[8] C. Hagner,[51] F. Handa,[43] T. Hara,[30] K. Hasuko,[34] H. Hayashii,[23] M. Hazumi,[8] I. Higuchi,[43] L. Hinz,[18] T. Hokuue,[22] Y. Hoshi,[42] W.-S. Hou,[25] Y. B. Hsiung,[25] H.-C. Huang,[25] T. Igaki,[22] Y. Igarashi,[8] T. Iijima,[22] K. Inami,[22] A. Ishikawa,[22] R. Itoh,[8] H. Iwasaki,[8] Y. Iwasaki,[8] H. K. Jang,[37] J. H. Kang,[53] J. S. Kang,[15] P. Kapusta,[26] S. U. Kataoka,[23] N. Katayama,[8] H. Kawai,[2] T. Kawasaki,[28] H. Kichimi,[8] D. W. Kim,[38] H. J. Kim,[53] H. O. Kim,[38] Hyunwoo Kim,[15] J. H. Kim,[38] S. K. Kim,[37] K. Kinoshita,[4] S. Kobayashi,[35] S. Korpar,[20,13] P. Križan,[19,13] P. Krokovny,[1] R. Kulasiri,[4] S. Kumar,[31] A. Kuzmin,[1] Y.-J. Kwon,[53] J. S. Lange,[5,34] G. Leder,[11] S. H. Lee,[37] J. Li,[36] S.-W. Lin,[25] D. Liventsev,[12] R.-S. Lu,[25] J. MacNaughton,[11] G. Majumder,[40] F. Mandl,[11] D. Marlow,[33] T. Matsuishi,[22] S. Matsumoto,[3] T. Matsumoto,[46] W. Mitaroff,[11] K. Miyabayashi,[23] H. Miyake,[30] H. Miyata,[28] G. R. Moloney,[21] T. Mori,[3] T. Nagamine,[43] Y. Nagasaka,[9] T. Nakadaira,[44] E. Nakano,[29] M. Nakao,[8] J. W. Nam,[38] Z. Natkaniec,[26] S. Nishida,[16] O. Nitoh,[47] S. Noguchi,[23] T. Nozaki,[8] S. Ogawa,[41] T. Ohshima,[22] T. Okabe,[22] S. Okuno,[14] S. L. Olsen,[7] Y. Onuki,[28] H. Ozaki,[8] P. Pakhlov,[12] H. Palka,[26] C. W. Park,[15] H. Park,[17] K. S. Park,[38] L. S. Peak,[39] J.-P. Perroud,[18] L. E. Piilonen,[51] F. J. Ronga,[18] M. Rozanska,[26] K. Rybicki,[26] H. Sagawa,[8] S. Saitoh,[8] Y. Sakai,[8] T. R. Sarangi,[50] M. Satapathy,[50] A. Satpathy,[8,4] O. Schneider,[18] S. Schrenk,[4] J. Schümann,[25] C. Schwanda,[8,11] S. Semenov,[12] K. Senyo,[22] R. Seuster,[7] M. E. Sevior,[21] H. Shibuya,[41] V. Sidorov,[1] J. B. Singh,[31] S. Stanič,[8,*] M. Starič,[13] A. Sugi,[22] A. Sugiyama,[22] K. Sumisawa,[8] T. Sumiyoshi,[46] S. Suzuki,[52] S. Y. Suzuki,[8] T. Takahashi,[29] F. Takasaki,[8] K. Tamai,[8] N. Tamura,[28] J. Tanaka,[44] M. Tanaka,[8] G. N. Taylor,[21] Y. Teramoto,[29] S. Tokuda,[22] T. Tomura,[44] K. Trabelsi,[7] T. Tsuboyama,[8] T. Tsukamoto,[8] S. Uehara,[8] K. Ueno,[25] Y. Unno,[2] S. Uno,[8] G. Varner,[7] K. E. Varvell,[39] C. C. Wang,[25] C. H. Wang,[24] J. G. Wang,[51] M.-Z. Wang,[25] Y. Watanabe,[45] E. Won,[15] B. D. Yabsley,[51] Y. Yamada,[8] A. Yamaguchi,[43] Y. Yamashita,[27] Y. Yamashita,[44] M. Yamauchi,[8] H. Yanai,[28] M. Yokoyama,[44] Y. Yuan,[10] Y. Yusa,[43] C. C. Zhang,[10] Z. P. Zhang,[36] Y. Zheng,[7] V. Zhilich,[1] and D. Žontar[19,13]

(Belle Collaboration)

[1]*Budker Institute of Nuclear Physics, Novosibirsk*
[2]*Chiba University, Chiba*
[3]*Chuo University, Tokyo*
[4]*University of Cincinnati, Cincinnati, Ohio 45221*
[5]*University of Frankfurt, Frankfurt*
[6]*Gyeongsang National University, Chinju*
[7]*University of Hawaii, Honolulu, Hawaii 96822*
[8]*High Energy Accelerator Research Organization (KEK), Tsukuba*
[9]*Hiroshima Institute of Technology, Hiroshima*
[10]*Institute of High Energy Physics, Chinese Academy of Sciences, Beijing*
[11]*Institute of High Energy Physics, Vienna*
[12]*Institute for Theoretical and Experimental Physics, Moscow*
[13]*J. Stefan Institute, Ljubljana*
[14]*Kanagawa University, Yokohama*
[15]*Korea University, Seoul*
[16]*Kyoto University, Kyoto*
[17]*Kyungpook National University, Taegu*
[18]*Institut de Physique des Hautes Énergies, Université de Lausanne, Lausanne*
[19]*University of Ljubljana, Ljubljana*
[20]*University of Maribor, Maribor*
[21]*University of Melbourne, Victoria*
[22]*Nagoya University, Nagoya*
[23]*Nara Women's University, Nara*
[24]*National Lien-Ho Institute of Technology, Miao Li*
[25]*National Taiwan University, Taipei*
[26]*H. Niewodniczanski Institute of Nuclear Physics, Krakow*
[27]*Nihon Dental College, Niigata*
[28]*Niigata University, Niigata*
[29]*Osaka City University, Osaka*
[30]*Osaka University, Osaka*
[31]*Panjab University, Chandigarh*

[32]*Peking University, Beijing*
[33]*Princeton University, Princeton, New Jersey 08545*
[34]*RIKEN BNL Research Center, Upton, New York 11973*
[35]*Saga University, Saga*
[36]*University of Science and Technology of China, Hefei*
[37]*Seoul National University, Seoul*
[38]*Sungkyunkwan University, Suwon*
[39]*University of Sydney, Sydney NSW*
[40]*Tata Institute of Fundamental Research, Bombay*
[41]*Toho University, Funabashi*
[42]*Tohoku Gakuin University, Tagajo*
[43]*Tohoku University, Sendai*
[44]*University of Tokyo, Tokyo*
[45]*Tokyo Institute of Technology, Tokyo*
[46]*Tokyo Metropolitan University, Tokyo*
[47]*Tokyo University of Agriculture and Technology, Tokyo*
[48]*Toyama National College of Maritime Technology, Toyama*
[49]*University of Tsukuba, Tsukuba*
[50]*Utkal University, Bhubaneswer*
[51]*Virginia Polytechnic Institute and State University, Blacksburg, Virginia 24061*
[52]*Yokkaichi University, Yokkaichi*
[53]*Yonsei University, Seoul*

(Received 12 December 2002; published 18 March 2003)

We report a precise determination of the B^0-$\overline{B}^0$ mixing parameter Δm_d based on the time evolution of same-sign and opposite-sign dilepton yields in $\Upsilon(4S)$ decays. Data were collected with the Belle detector at KEKB. Using data samples of 29.4 fb^{-1} recorded at the $\Upsilon(4S)$ resonance and 3.0 fb^{-1} recorded at an energy 60 MeV below the resonance, we measure $\Delta m_d = [0.503 \pm 0.008(\text{stat}) \pm 0.010(\text{syst})]$ ps^{-1}. From the same analysis, we also measure the ratio of charged and neutral B meson production at the $\Upsilon(4S)$, $f_+/f_0 = 1.01 \pm 0.03(\text{stat}) \pm 0.09(\text{syst})$, and *CPT* violation parameters in B^0-$\overline{B}^0$ mixing, $\Re(\cos\theta) = 0.00 \pm 0.12(\text{stat}) \pm 0.01(\text{syst})$ and $\Im(\cos\theta) = 0.03 \pm 0.01(\text{stat}) \pm 0.03(\text{syst})$.

DOI: 10.1103/PhysRevD.67.052004 PACS number(s): 13.66.Bc, 13.25.Gv, 14.40.Gx

I. INTRODUCTION

The mass difference of the B^0-$\overline{B}^0$ mass eigenstates, Δm_d, is a fundamental parameter in the B meson system. The techniques that have been employed to measure it in $\Upsilon(4S) \rightarrow B^0\overline{B}^0$ decays fall into two categories: namely, inclusive and exclusive. Among the inclusive methods, the analysis of events where both B mesons decay into a final state that includes a high momentum lepton provides the largest event sample [1] and is well suited for further high precision measurements of the time evolution in the $B^0\overline{B}^0$ system. This system exhibits sensitivity not only to Δm_d, but also to other potentially interesting phenomena such as *CP* violation in mixing, the decay width difference between the two mass eigenstates and possible *CPT* violation in mixing [2].

Without the assumption of *CPT* invariance, the flavor and mass eigenstates of the neutral B mesons are related by

$$|B_H\rangle = p|B^0\rangle + q|\overline{B}^0\rangle,$$
$$|B_L\rangle = p'|B^0\rangle - q'|\overline{B}^0\rangle. \quad (1)$$

The coefficients p, q, p' and q' can be expressed in terms of the complex parameters θ and ϕ by $q/p = \tan(\theta/2)e^{i\phi}$ and $q'/p' = \cot(\theta/2)e^{i\phi}$. *CP* is violated if $\Im(\phi) \neq 0$, and *CPT* is violated if $\theta \neq \pi/2$ [2]. The time-dependent decay rates are given by [2]

$$\Gamma_{\Upsilon(4S)\rightarrow \ell^\pm\ell^\pm}(\Delta t) = \frac{|A_\ell|^4}{8\tau_{B^0}} e^{-|\Delta t|/\tau_{B^0}} |\sin\theta e^{\mp i\phi}|^2 \times \left[\cosh\left(\frac{\Delta\Gamma}{2}\Delta t\right) - \cos(\Delta m_d \Delta t)\right] \quad (2)$$

for same-sign (SS) dilepton events, and

$$\Gamma_{\Upsilon(4S)\rightarrow \ell^+\ell^-}(\Delta t) = \frac{|A_\ell|^4}{4\tau_{B^0}} e^{-|\Delta t|/\tau_{B^0}} \left\{ (1+|\cos\theta|^2)\cosh\left(\frac{\Delta\Gamma}{2}\Delta t\right) + (1-|\cos\theta|^2)\cos(\Delta m_d \Delta t) + 2\Re(\cos\theta)\sin\left(\frac{\Delta\Gamma}{2}\Delta t\right) - 2\Im(\cos\theta)\sin(\Delta m_d \Delta t)\right\} \quad (3)$$

*On leave from Nova Gorica Polytechnic, Nova Gorica.

for opposite-sign (OS) events. Here, we assume *CP* is conserved in the flavor specific semileptonic decay amplitudes of the neutral B mesons and set $A_\ell \equiv \langle X^- \ell^+ \nu_\ell | B^0 \rangle$ and $\overline{A}_\ell \equiv \langle X^+ \ell^- \overline{\nu}_\ell | \overline{B}^0 \rangle$ to be equal. Δm_d and $\Delta\Gamma$ are the differences in the mass and decay width between the two mass eigenstates of the neutral B meson, $\Gamma = 1/\tau_{B^0}$ is the average decay width of the two mass eigenstates, Δt is the proper time difference between the two B meson decays and is defined as $\Delta t \equiv t(\ell^+) - t(\ell^-)$ for the OS events, while the absolute value is taken for SS events.

In Eq. (2), *CP* violation appears as a difference in the $\ell^+\ell^+$ and $\ell^-\ell^-$ rates, in case of a non-zero $\Im(\phi)$. It does not depend on θ, $\Delta\Gamma$ or the fraction of mixed events. The last two terms in Eq. (3) are clearly asymmetric in Δt. The last term will dominate over the second-to-last term since $\Delta m_d \gg \Delta\Gamma$. In this analysis, we assume that $\Delta\Gamma$ and *CP* violating effects are negligibly small [3,4]. We extract Δm_d, f_+/f_0 the ratio of $\Upsilon(4S)$ branching fractions to B^+B^- and $B^0\overline{B}^0$, and the *CPT* violation parameters $\Re(\cos\theta)$ and $\Im(\cos\theta)$. Our previous determination of Δm_d using dilepton events from 5.9 fb^{-1} [1] treated f_+/f_0 as a fixed parameter. Otherwise the results reported here use the same analysis method and include the earlier data and, therefore, supersede the previous values.

II. EVENT SELECTION

The Belle detector, which consists of a silicon vertex detector (SVD), a central drift chamber (CDC), aerogel Čerenkov counters (ACC), time-of-flight counters, an electromagnetic calorimeter (ECL), and a muon and K_L detector (KLM), is described in detail elsewhere [5]. For electron identification, we use position, cluster energy, and shower shape in the ECL, combined with track momentum and dE/dx in the CDC and hits in the ACC. For muon identification, we extrapolate the CDC track to the KLM and compare the measured range and transverse deviation in the KLM with the expected values.

A. Lepton selection

The efficiencies for identifying leptons are determined from two-photon process data samples: $e^+e^- \to e^+e^-e^+e^-$ for electrons and $e^+e^- \to e^+e^-\mu^+\mu^-$ for muons. For both cases, the possible degradation of efficiency due to nearby tracks that are not present in QED events but must be considered in hadronic events is examined using special hadronic event data samples that contain embedded Monte Carlo (MC) lepton tracks.

We determine the probabilities for misidentifying hadrons as leptons using data samples of $K_S \to \pi^+\pi^-$ decays for pions, $\phi \to K^+K^-$ decays for kaons, and $\Lambda \to p\pi^-$ decays for protons. For tracks in the kinematic region of the dilepton event selection, the identification efficiencies are 92.6% for electrons and 87.0% for muons. About 0.1% of pions and kaons, 0.2% of protons and 1.2% of antiprotons are misidentified as electrons. About 1% of pions and kaons, and 0.2% of protons and antiprotons are misidentified as muons.

TABLE I. Summary of dilepton events after all cuts. The numbers in the off-resonance columns are scaled using the luminosity ratio and represent the contribution included in the on-resonance data.

Lepton flavors	On resonance		Off resonance	
	SS	OS	SS	OS
ee	9877	52141	107.4	1513.3
$\mu\mu$	15503	65435	1464.4	4451.9
$e\mu$	24458	113305	976.3	4403.1
Total	49838	230881	2548.1	10368.2

B. Hadronic event selection

Hadronic events are selected from a data set corresponding to 29.4 fb^{-1} at the $\Upsilon(4S)$ resonance and 3.0 fb^{-1} at an energy 60 MeV below the peak. Hadronic events are required to have at least five tracks, an event vertex with radial and z coordinates (where the z axis passes through the nominal interaction point, and is antiparallel to the positron beam) within 1.5 cm and 3.5 cm respectively of the nominal interaction point (IP), a total reconstructed center-of-mass (c.m.) energy greater than $0.5W$ [W is the $\Upsilon(4S)$ c.m. energy], a z component of the net reconstructed c.m. momentum less than $0.3W/c$, a total ECL energy deposit between $0.025W$ and $0.9W$, and a ratio R_2 of the second and zeroth Fox-Wolfram moments [6] less than 0.7.

C. Dilepton event selection

Lepton candidates are selected from charged tracks that have a distance of closest approach to the run-dependent IP less than 0.05 cm radially ($dr_{\rm IP}$) and 2.0 cm in z ($dz_{\rm IP}$). At least one r-ϕ and two z hits are required in the SVD. To eliminate electrons from $\gamma \to e^+e^-$ conversions, electron candidates are paired with all other oppositely charged tracks and the invariant mass (assuming the electron mass hypothesis) $M_{e^+e^-}$ is calculated. If $M_{e^+e^-} < 100$ MeV/c^2, the candidate electron is rejected. If a hadronic event contains more than two lepton candidates, we use the two candidates with the highest c.m. momenta.

The c.m. momentum of each lepton is required to be in the range $1.1\ {\rm GeV}/c < p^* < 2.3\ {\rm GeV}/c$. The lower cut reduces contributions from secondary (charm) decay. The upper cut reduces the contribution from non-$B\overline{B}$ continuum events. The angle of each lepton track with respect to the z axis in the laboratory frame must satisfy $30° < \theta_{\rm lab} < 135°$. This cut rejects tracks with large angles of incidence in the SVD and hence provides better z vertex resolution. In addition, these cuts remove lepton candidates whose particle identification is performed using the endcap KLM or ECL, where the performance is not as good as that of the barrel sections. Events that contain one or more J/ψ candidates are rejected. We calculate the invariant mass of each candidate lepton with each oppositely charged track (assuming the correct lepton mass hypothesis). If the invariant mass falls into the J/ψ region, defined as $-0.15\ {\rm GeV}/c^2 < (M_{e^+e^-} - M_{J/\psi}) < 0.05\ {\rm GeV}/c^2$, $-0.05\ {\rm GeV}/c^2 < (M_{\mu^+\mu^-} - M_{J/\psi}) < 0.05\ {\rm GeV}/c^2$, the candidate event is rejected. The looser

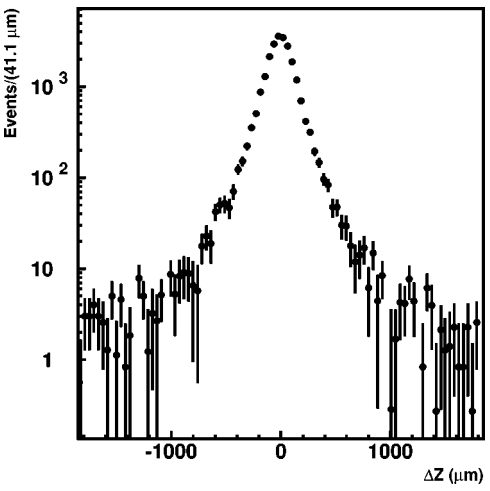

FIG. 1. Detector response function determined from the J/ψ data.

lower cut for the electron pair invariant mass is to reject J/ψ mesons whose calculated mass is low due to bremsstrahlung of the daughter electron(s). The opening angle of the two leptons in the c.m. frame $\theta^*_{\ell\ell}$, is required to satisfy $-0.8 < \cos\theta^*_{\ell\ell} < 0.95$ to reduce jet-like continuum events, SS events where the two reconstructed tracks originate from the same particle and events with a primary lepton and a secondary lepton originating from the same B meson. After all cuts are applied, we obtain 49838 SS and 230881 OS events. The numbers of selected dilepton events are summarized in Table I.

III. Δz DETERMINATION

The z coordinate of each B meson decay vertex is determined from the intersection of the lepton track with the run-dependent profile of the IP smeared in the $r-\phi$ plane by 21 μm to account for the transverse B flight length. We define the difference between the z coordinates of the two leptons as $\Delta z = z(\ell^+) - z(\ell^-)$ for OS events and $\Delta z = |z(\ell^\pm) - z(\ell^\pm)|$ for SS events. Δz is related to the proper-time difference by $\Delta z \simeq c\beta\gamma\Delta t$. The Lorentz boost factor of the e^+e^- c.m. frame at KEKB is $\beta\gamma = 0.425$ [7].

The observed Δz distributions have contributions from "signal" defined as events where both leptons are primary leptons from semileptonic decays of B mesons, and "background" where at least one lepton is secondary or fake, or the event is from the continuum. The contributions from "signal" are theoretically well-defined distributions convolved with the detector response function, which describes the difference between the true Δz and the measured Δz. In order to estimate the detector response function, we employ J/ψ decays, where the true Δz is equal to zero, and whose measured Δz distribution, after the contribution of background is subtracted, yields the response function.

Candidate J/ψ events are selected using the same criteria as the dilepton sample except the J/ψ veto and the cuts on $\cos\theta^*_{\ell\ell}$ are not applied. We define the J/ψ signal region as $3.00\ \mathrm{GeV}/c^2 < M_{e^+e^-} < 3.14\ \mathrm{GeV}/c^2$ and $3.05\ \mathrm{GeV}/c^2 < M_{\mu^+\mu^-} < 3.14\ \mathrm{GeV}/c^2$, and the sideband region as $3.18\ \mathrm{GeV}/c^2 < M_{\ell^+\ell^-} < 3.50\ \mathrm{GeV}/c^2$ for both electrons and muons. A linear function is fitted to the sideband region of the mass distribution and extrapolated to the signal region. Using the fit result, we scale the Δz distribution in the sideband region to the background underneath the peak in the signal region, and subtract it from the signal region Δz distribution. Figure 1 shows the resulting detector response function. It has rms $= 186$ μm in the range $|\Delta z| < 1850$ μm. We use this histogram as a lookup table in the analysis.

IV. FITTING

The mixing parameter Δm_d and other parameters are extracted by simultaneously fitting the Δz distributions of SS and OS events to the sum of contributions from all known signal and background sources. We use a binned maximum likelihood method. The background Δz distributions are obtained from MC simulations and used in the fits in the form of lookup tables.

A. Signal Δz distributions

The signal from the neutral B meson pairs originates either from $B^0\overline{B}^0$ (unm) or from B^0B^0 and $\overline{B}^0\overline{B}^0$ (mix). If *CPT* is assumed to be conserved, the signal distributions are expressed by

$$P^{\mathrm{unm}} = N_{4S} f_0 b_0^2 \epsilon^{\mathrm{unm}}_{\ell\ell} \frac{e^{-|\Delta t|/\tau_{B^0}}}{4\tau_{B^0}} [1 + \cos(\Delta m_d \Delta t)],$$

$$P^{\mathrm{mix}} = N_{4S} f_0 b_0^2 \epsilon^{\mathrm{mix}}_{\ell\ell} \frac{e^{-|\Delta t|/\tau_{B^0}}}{4\tau_{B^0}} [1 - \cos(\Delta m_d \Delta t)]. \tag{4}$$

If the possibility of *CPT* violation is included, these expressions become

$$P^{\mathrm{unm}} = N_{4S} f_0 b_0^2 \epsilon^{\mathrm{unm}}_{\ell\ell} \frac{e^{-|\Delta t|/\tau_{B^0}}}{4\tau_{B^0}} [(1 - |\cos\theta|^2)\cos(\Delta m_d \Delta t) + 1 + |\cos\theta|^2 - 2\Im(\cos\theta)\sin(\Delta m_d \Delta t)]$$

$$P^{\mathrm{mix}} = N_{4S} f_0 b_0^2 \epsilon^{\mathrm{mix}}_{\ell\ell} \frac{e^{-|\Delta t|/\tau_{B^0}}}{4\tau_{B^0}} |\sin\theta|^2 [1 - \cos(\Delta m_d \Delta t)]. \tag{5}$$

The integrals of P^{unm} and P^{mix} give the time-integrated fraction of mixed events

$$\chi_d = \frac{|\sin\theta|^2 x_d^2}{|\sin\theta|^2 x_d^2 + 2 + x_d^2 + |\cos\theta|^2 x_d^2} \tag{6}$$

where $x_d \equiv \tau_{B^0} \Delta m_d$. When *CPT* is conserved, this becomes the more familiar expression $\chi_d = x_d^2/(2 + 2x_d^2)$. The values of $|\cos\theta|^2$ and $|\sin\theta|^2$ are determined from $\Re(\cos\theta)$ and $\Im(\cos\theta)$.

The signal distribution for charged B meson pairs is the same for both the *CPT* conserving and *CPT* violating cases and is given by

TABLE II. Results of fits. $n_{\rm DF}$ is the number of degrees of freedom.

Fitting method	*CPT* conserved	Allow *CPT* violation
Δm_d (ps^{-1})	0.503 ± 0.008	0.503 ± 0.008
f_+ / f_0	1.01 ± 0.03	1.02 ± 0.03
$\Re(\cos\theta)$		0.00 ± 0.12
$\Im(\cos\theta)$		0.03 ± 0.01
T_{CT}	94 ± 6	91 ± 5
T_{WT}	140 ± 2	139 ± 2
χ^2	139 ($n_{\rm DF}=86$)	132 ($n_{\rm DF}=84$)

$$P^{\rm chd} = N_{4S} f_+ b_+^2 \epsilon_{\ell\ell}^{\rm chd} \frac{e^{-|\Delta t|/\tau_{B^+}}}{2\tau_{B^+}}. \quad (7)$$

In the equations above, N_{4S} is the total number of $\Upsilon(4S)$ events, f_0 and f_+ are the branching fractions of $\Upsilon(4S)$ to neutral and charged B pairs ($f_+ + f_0 = 1$), b_0 and b_+ are the semileptonic branching fractions for neutral and charged B mesons, $\epsilon_{\ell\ell}$ with superscript are the efficiencies for selecting dilepton events of charged (chd), unmixed (unm), and mixed (mix) origins. The ratio $\epsilon_{\ell\ell}^{\rm chd} : \epsilon_{\ell\ell}^{\rm unm} : \epsilon_{\ell\ell}^{\rm mix}$ is determined from MC simulations and is fixed in the fit, because any detector effect that is not simulated correctly should affect events with these origins equally. The Δz distributions are obtained from these distributions [Eqs. (4), (5) and (7)] by conversion from Δt and convolution with the emperical resolution function described in the previous section.

B. Background Δz distributions

The background Δz distributions are estimated using the MC simulations. A comparison of the Δz distribution of J/ψ data samples between the data and MC simulations shows that the data distribution is wider than the MC distribution. A detailed study showed that after convolving the MC distribution with a $\sigma = 50 \pm 18$ μm Gaussian, the distributions compared favourably. We smear MC background distributions in the same way to compensate for this discrepancy.

We categorize the backgrounds into eight types depending on their sources: charged B pairs, mixed and unmixed neutral B pairs, and continuum, each of them contributing to both SS and OS events. To normalize the amount of continuum background, we use the off-resonance data. This leaves seven parameters to normalize the fractions of other backgrounds. The first of these is χ_d which is varied in the fit as given by Eq. (6); the remaining six are associated with the efficiencies for selecting these background events which are denoted as

$$\epsilon_{SS}^{\rm chd}, \quad \epsilon_{OS}^{\rm chd}, \quad \epsilon_{SS}^{\rm unm}, \quad \epsilon_{OS}^{\rm unm}, \quad \epsilon_{SS}^{\rm mix}, \quad \epsilon_{OS}^{\rm mix}. \quad (8)$$

We combine these six types into two: correct tag (CT) which is associated with $\epsilon_{OS}^{\rm chd}$, $\epsilon_{OS}^{\rm unm}$, $\epsilon_{SS}^{\rm mix}$, and wrong tag (WT) which is associated with $\epsilon_{SS}^{\rm chd}$, $\epsilon_{SS}^{\rm unm}$, $\epsilon_{OS}^{\rm mix}$. For both CT and WT backgrounds, relative fractions of the three background types are fixed according to the MC simulations. We then determine the Δz distributions for CT and WT backgrounds by adding the three corresponding contributions.

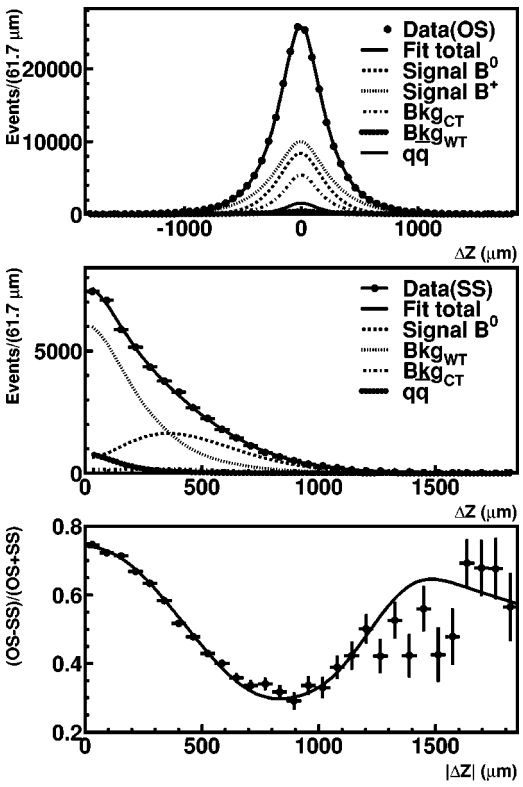

FIG. 2. Results of the simultaneous fit to the same-sign and opposite-sign Δz distributions assuming *CPT* invariance. The upper two plots are for the opposite-sign and same-sign events, respectively. Signal and background obtained from the fit are also shown. The bottom plot is the OS-SS asymmetry with the fit result superimposed.

The shapes of the Δz background distributions and the normalization of the backgrounds from neutral B events depend on Δm_d. To account for this, we generated two samples of generic neutral B MC events, one with $\Delta m_d = 0.469$ ps^{-1} and one with $\Delta m_d = 0.522$ ps^{-1}. Background Δz distributions for any value of Δm_d are produced by linear interpolation between these two MC data sets.

The MC simulation does not always reproduce the hadron showering processes correctly in the kinematic region of interest. In order to account for possible discrepancies, we obtain an overall correction factor by using a special control data sample. In this sample events are selected in the same way as the dilepton events, except that we now require that exactly one lepton passes the lepton selection criteria and the other track passes all selection criteria except for the lepton identification requirements. The ratio of data to MC simulations fake rates binned in $\theta_{\rm lab}$ and p is then applied to the control sample to obtain the overall fake rates for the dilepton analysis. From this method, the hadron misidentification probabilities of the MC simulations are increased by 6% for muons and decreased by 5% for electrons.

V. RESULTS

In the fit, we fix the parameters $\tau_{B^0} = 1.542 \pm 0.016$ ps, and $\tau_{B^+}/\tau_{B^0} = 1.083 \pm 0.017$ [3], and we impose the con-

TABLE III. Systematic errors contributing to the Δm_d and f_+/f_0 measurements.

Source	Δm_d (ps^{-1})	f_+/f_0
τ_{B^+}/τ_{B^0} (± 0.017)	± 0.0053	± 0.071
Detector response function	± 0.0047	± 0.021
Monte Carlo statistics	± 0.0036	± 0.011
50 μm smearing of background Δz (± 18 μm)	± 0.0032	± 0.015
Δz cut	± 0.0030	± 0.010
$\theta_{\rm lab}$ cut	± 0.0030	± 0.030
τ_{B^0} (± 0.016 ps)	± 0.0012	± 0.002
$dr_{\rm IP}$ cut	± 0.0010	± 0.003
Continuum contribution	± 0.0008	± 0.001
BR($B\to DX$)(D^0:$\pm 4.7\%$,D^+:$\pm 7.9\%$)	± 0.0007	± 0.001
Fake rate correction (μ:$\pm 3\%$,e:$\pm 25\%$)	± 0.0007	± 0.002
Linear interpolation	± 0.0005	± 0.020
IP profile (± 10 μm)	± 0.0002	± 0.005
Quadratic sum	± 0.0097	± 0.086

straint $b_+/b_0 = \tau_{B^+}/\tau_{B^0}$. In the fit where *CPT* is conserved, we have a total of five parameters to be fitted. They are Δm_d, f_+/f_0, two parameters which are related to the fractions of CT and WT backgrounds and are expressed as $T_{CT} \equiv b_+^2 \epsilon_{\ell\ell}^{\rm chd}/\epsilon_{OS}^{\rm chd}$ and $T_{WT} \equiv b_+^2 \epsilon_{\ell\ell}^{\rm chd}/\epsilon_{SS}^{\rm chd}$, and an overall normalization. In the search for *CPT* violation, we add two parameters $\Re(\cos\theta)$ and $\Im(\cos\theta)$. The results of the fits are summarized in Table II.

The values of Δm_d and f_+/f_0 do not vary in a significant way when *CPT* violation is included. We use the result from the *CPT* conserving fit to obtain Δm_d and f_+/f_0. The Δz distributions for the SS and OS events and the resulting asymmetry are shown in Fig. 2, together with the fit results.

Systematic errors in the determination of Δm_d and f_+/f_0 include contributions from uncertainties in the parameters that are fixed in the fit: τ_{B^+}/τ_{B^0}, the extra 50 μm smearing of the background Δz distributions, τ_{B^0}, inclusive D meson branching fractions $B\to D^+X$ and $B\to D^0X$. Also contributing to the systematic errors are uncertainties in the continuum contribution determined from off-resonance data, lepton misidentification probabilities, detector response function, MC statistics, background function linear interpolation end points, IP profile smearing, the event selection criteria $\theta_{\rm lab}$ and $dr_{\rm IP}$, and the Δz fit range. Uncertainties of the overall z scale in the detector and the boost factor $\beta\gamma$ can also contribute to the systematic error.

The contribution from the detector response function is dominated by the statistics of the J/ψ event sample. Biases due to approximating the detector response function with the Δz distribution of J/ψ events and the effect of the B motion in the $\Upsilon(4S)$ frame also have some contribution. We estimate the uncertainty of the detector response function by comparing the results of fits to a full MC simulation using three different types of response functions. These are the J/ψ response function (extracted in the same way as in data), a true Δz response function, and a response function based on the proper time difference between the B meson decays (for systematic errors associated with the B motion in the $\Upsilon(4S)$ frame). The true Δz response function is constructed using signal events and subtracting the true Δz from the measured Δz. The proper time response function is constructed in the same manner, except the true $\beta\gamma c\Delta t$ is subtracted. Each of the three types of response functions is generated using 35 independent MC data sets, resulting in 105 response functions. The fit results using each response function are then compared to extract the systematic errors. Additionally we vary the amount of background subtraction from the J/ψ mass peak by ± 1 σ, and repeat the fits. The final detector response function systematic error is the combined error resulting from the above methods.

To quantify the systematic error associated with the MC statistics, the MC data are divided into $n=20$ sets and the data are fitted using each background distribution P_i ($i=1,...,n$). Both the shapes and the efficiency ratios are independent for each fit. The fits were repeated with 45 different pairs of end points for the Δm_d linear interpolation. The rms of the fit results was assigned as the error. The systematic error for the IP constraint was estimated by varying the smearing used to represent the transverse B flight length by ± 10 μm. The cuts on the variables Δz, $\theta_{\rm lab}$ and $dr_{\rm IP}$ were varied in the region of their default values and the changes in the fit results assigned as errors. The remaining systematic errors were calculated by varying the default values by ± 1 σ, repeating the fits and assigning the differences as errors. The contributions from the uncertainties in the z scale and $\beta\gamma$ were found to be negligible.

The errors are summarized in Table III.

To reduce the backgrounds, the analysis was repeated with tighter p^* cuts, and separate fits were performed with ee, $e\mu$ and $\mu\mu$ sub-samples. Deviations from the default results were all consistent with statistical fluctuations. We repeated the fit including the effects of $\Delta\Gamma/\Gamma = 1\%$ and found the shift in results to be negligible (≈ 0.0001 ps^{-1}).

The largest contributions to the systematic error for $\Im(\cos\theta)$ come from the uncertainty in the extra 50 μm smearing and the $\theta_{\rm lab}$ selection criteria and amount to ± 0.03. The systematic error for $\Re(\cos\theta)$ is dominated by the uncer-

tainty in the response function. We conservatively assign an error of ± 0.01.

In summary, we obtain

$$\Delta m_d = [0.503 \pm 0.008(\text{stat}) \pm 0.010(\text{syst})]\,\text{ps}^{-1},$$

$$f_+/f_0 = 1.01 \pm 0.03(\text{stat}) \pm 0.09(\text{syst}),$$

$$\Re(\cos\theta) = 0.00 \pm 0.12(\text{stat}) \pm 0.01(\text{syst}),$$

$$\Im(\cos\theta) = 0.03 \pm 0.01(\text{stat}) \pm 0.03(\text{syst}). \quad (9)$$

Using world averages for Δm_d, the neutral B meson mass and decay width [3], these *CPT* parameters imply [2] the upper limits $|m_{B^0} - m_{\overline{B}^0}|/m_{B^0} < 1.16 \times 10^{-14}$ and $|\Gamma_{B^0} - \Gamma_{\overline{B}^0}|/\Gamma_{B^0} < 0.11$ at 90% C.L.

VI. SUMMARY

In summary, we have measured Δm_d and the ratio of branching fractions for $\Upsilon(4S)$ decay to B^+B^- and $B^0\overline{B}^0$, f_+/f_0, using inclusive dilepton events. The largest contributions to the systematic error for the Δm_d measurement come from the response function and the uncertainty in the B meson lifetime ratio τ_{B^+}/τ_{B^0}. Recent measurements [3] of this lifetime ratio have significantly reduced this systematic contribution since our first measurement [1]. The result of this dilepton analysis $\Delta m_d = (0.503 \pm 0.008 \pm 0.010)\ \text{ps}^{-1}$ is in good agreement with the results from other methods used by Belle [8] and the current world average [3]. The error for the f_+/f_0 measurement is dominated by the uncertainty in τ_{B^+}/τ_{B^0}. We have also obtained new limits on *CPT* violation parameters.

ACKNOWLEDGMENTS

We wish to thank the KEKB accelerator group for the excellent operation of the KEKB accelerator. We acknowledge support from the Ministry of Education, Culture, Sports, Science, and Technology of Japan and the Japan Society for the Promotion of Science; the Australian Research Council and the Australian Department of Industry, Science and Resources; the National Science Foundation of China under Contract No. 10175071; the Department of Science and Technology of India; the BK21 program of the Ministry of Education of Korea and the CHEP SRC program of the Korea Science and Engineering Foundation; the Polish State Committee for Scientific Research under Contract No. 2P03B 17017; the Ministry of Science and Technology of the Russian Federation; the Ministry of Education, Science and Sport of the Republic of Slovenia; the National Science Council and the Ministry of Education of Taiwan; and the U.S. Department of Energy.

[1] Belle Collaboration, K. Abe *et al.*, Phys. Rev. Lett. **86**, 3228 (2001); BABAR Collaboration, B. Aubert *et al.*, *ibid.* **88**, 221803 (2002).
[2] See, for example, A. Mohapatra, M. Satpathy, K. Abe, and Y. Sakai, Phys. Rev. D **58**, 036003 (1998), and references therein.
[3] Particle Data Group, K. Hagiwara *et al.*, Phys. Rev. D **66**, 010001 (2002).
[4] BABAR Collaboration, B. Aubert *et al.*, Phys. Rev. Lett. **88**, 231801 (2002).
[5] Belle Collaboration, A. Abashian *et al.*, Nucl. Instrum. Methods Phys. Res. A **479**, 117 (2002).
[6] G. C. Fox and S. Wolfram, Phys. Rev. Lett. **41**, 1581 (1978).
[7] KEK Report No. 2001-157, 2001.
[8] Belle Collaboration, T. Tomura *et al.*, Phys. Lett. B **524**, 207 (2002); Belle Collaboration, K. Hara *et al.*, Phys. Rev. Lett. **89**, 251803 (2002).